RESEARCH REPORT

VTT-R-01091-20

Characteristics of crushed battery waste and mechanical pre-treatment at laboratory scale

Authors: John Bachér, Tuomo Mäkelä, Antti Porvali, Lotta Rintala

Confidentiality: Public

Report's title	
Characteristics of crushed battery waste and mechanical pre-treatment at laboratory scale	
Project name	**Date, Place**
BATCircle	5.5.2021, Espoo
Author(s)	**Pages**
John Bachér, Tuomo Mäkelä, Antti Porvali, Lotta Rintala	17
Keywords	**Report identification code**
Battery recycling, characterization, mechanical treatment	VTT-R-01091-20

Summary

The study aimed at investigating the characteristics and mechanical processability of primary crushed E-bike and power tool batteries. Both samples, the e-bike and power tool, were sieved into 12 fractions (Sieve sizes of 0.5 – 63 mm) with rather similar size distribution. Gas emissions from all the fractions were also monitored with FTIR, and HF detector was used to identify HF. No HF was detected, but carbon emissions (e.g. CO2) were detected from the sample fractions. After emission tests, the power tool sample was discarded, and the study was refocused on the E-bike sample which was divided into two parts (composed of individual size fraction) and were further inspected. The < 4 mm fractions were analysed separately with XRF, and the results treated in aggregate indicated the presence of NMC-111 type cathode materials. The size fractions > 4 mm were visually inspected for classification as well as liberation purposes. Significantly, undamaged cells were detected due to the primary crushing. In particular, poor liberation was identified upon Al cathode foils, which is expected due to the polymeric binders. The mechanical treatment experiments showed that significant share of damaged battery cells was removed with magnetic separation whereas cathode and anode as well as plastics continued to eddy current separation. Eddy current enriched anode and cathode particles to splitter fraction, the recoveries were 32 and 28 wt% respectively. This study concentrated on preliminary suitability of the eddy current separation on crushed battery wastes. Despite the rather low recoveries, a separation property of anode and cathode particles was observed with eddy current. In this task, the raw material was only primary crushed, the foils were not fully liberated, which decreases the recoveries.

Confidentiality	Public

VTT's contact address
john.bacher@vtt.fi

Contents

Contents....2

Introduction....3

Materials and methods....4

- Bulk Sample Treatment....4
- Size Fraction Analyses....6
- Magnetic and Eddy-Current Separation....7

Results and Discussion....8

- Size Classification....8
- Material Composition and Distribution....9
- Gas Measurements....13
- Magnetic and Eddy-Current Separation....14

Conclusions....16

Acknowledgement....16

References....17

Introduction

Secondary lithium-ion (Li-ion) batteries have been adopted in a wide variety of different applications. Presently, they have been positioned to be a vital piece of device that will, in part, enable electrification of transportation and reduce reliance on combustion engine and its associated products. Production of Li-ion batteries has expanded rapidly. Because a significant portion of a Li-ion battery cell contains valuable metals, such as Ni, Co, Mn and Li, the industry and society alike have woken to the limitations in supply of non-renewable resources to which battery minerals belong. This is exemplified by the recent European Commission classification of critical elements, to which Li, Co and battery-applicable graphite belong to [1]. If the Ni-Mn-Co –containing batteries are the technology around which the electrification of the transportation will evolve, it will necessitate further mining and refining operations. Similarly, it has been predicted that recycling would have an important role, both from the perspective of not wasting the non-renewable resources, as well as from the perspective of lessening the impact on supply chain by circulating the spent batteries as raw materials back to the production chain.

Recycling of Li-ion batteries starts from collection, and possibly sorting, depending on the product and its source. It can be easier to collect e.g. automotive batteries and keep them separate from other types than smaller consumer grade secondary batteries. Once batteries have been recovered, the first step is the neutralization of the electric charge within the battery, followed up by dismantling of larger battery packs. After dismantling, the options become more complex as to how to proceed. Many recycling operators have opted for mechanical treatment: comminution, followed up by varied set of unit processes that aim at recovery of graphite, electrolyte, transition metal oxides (TMOs), fluoride compounds, metal electrode foils and more. Packing complex material technology in a limited, small space greatly influences the difficulty of creating a recycling process that is concurrently economic, efficient and safe.

Initially, the research on recycling processes appear familiar as traditional mineral unit processes were utilized in the recycling as well. Similarly, in this study, size-based separation (sieving), magnetic and eddy-current separation was investigated. Size-based separation after comminution has been investigated academically [2]–[4] as well as implemented in industrial recycling processes widely [5]. In modern secondary batteries the cathode and anode materials are often mono or polycrystalline powders: in Li-ion batteries, these include different lithium transition metal oxides, lithium transition metal phosphates and more, mixed with graphite [6]. Anode consists of anode grade spheroid graphite. In principle, this could allow their size-based separation from large pieces such as cathode and anode foils made of Al and Cu, respectively as well as from other larger pieces, such as casings. In practice, the situation is more difficult as the mechanical pre-treatment is violent and non-selective, causing creation of smaller pieces of foil that contaminate these finer fractions [4]. Furthermore, this is not all: unlike ordinary Ni and Co minerals, batteries contain various organic compounds, such as volatile organic electrolytes as well as polymeric binder that is mixed with the cathode powders in order to attach the electrode powder slurry on electrode foils. Aiming to better liberation of the powders, academic and industrial actors have explored both thermal and chemical pre-treatments to either decompose or chemically dissolve the binder, respectively. In our present study, the binder will not be removed or treated. After size-based separation and before or after potential thermal treatments, magnetic separation can be performed. Magnetic separation is utilized by many battery recycling companies, including AkkuSer [7]. This is useful in separation of the casings which are commonly made of steel currently. However, incomplete comminution may hinder magnetic separation if sufficient liberation of powders is not achieved. It also needs to be noted that Al casings have also been reportedly used in the past, which are not magnetic [8]. Finally, eddy-current separation was investigated in the present study. Eddy-current separation is less commonly utilized in published academic or industrial recycling processes. Eddy-current separation is a method that utilizes dia- and paramagnetism of certain

materials, such as the Al and Cu foils, to separate them from materials devoid of magnetic properties. However, it might be challenging to apply this method due to the cathode slurry being binder enhanced. It has been shown that Co losses occur along with Al foils, exemplifying that simple crushing alone will not sufficiently liberate cathode powders from cathode foils [4]. In order to solve this problem, several researchers and organizations have attempted to utilize thermal decomposition [9] of PVDF, solvents such as n-methylpyrrolidone (NMP) [10] and even more advanced and complicated mechanical treatment steps, involving impacts on material, airflow classification and more to liberate the powders from the foils [2], [11], [12].

Task 3.1 “Mechanical treatment of waste EV- batteries” of the BATCircle project aimed at investigating the “mineralogy” of spent rechargeable batteries with an outlook of EV batteries particles to be used as feed in later metallurgical transformation stages. In this task, Li-ion batteries, provided by Akkuser, were processed. Two pre-crushed samples was received: an e-bike sample and a power tool sample. The goal of the task was two-pronged: I) learn about the safety-related issues in handling of batteries that have been violently opened and II) determine how a certain mechanical processing scheme could be applied to the said fractions. First, size-based separation by sieving was performed, followed by hand classification of components to determine the material composition of the sample. Based on the composition analysis, the overflow of certain size was subjected to magnetic and eddy-current separation. The underflow was characterized for chemical composition. Hand-classification was repeated for the magnetic and eddy-current separation process products.

Materials and methods

Bulk Sample Treatment

Two separate, primary crushed samples of Li-ion batteries were received from AkkuSer Oy. The first sample, weighing in 31 kg, originated from E-bikes, and the second sample, weighing in 29 kg, from power tools. The samples are depicted in Figure 1.

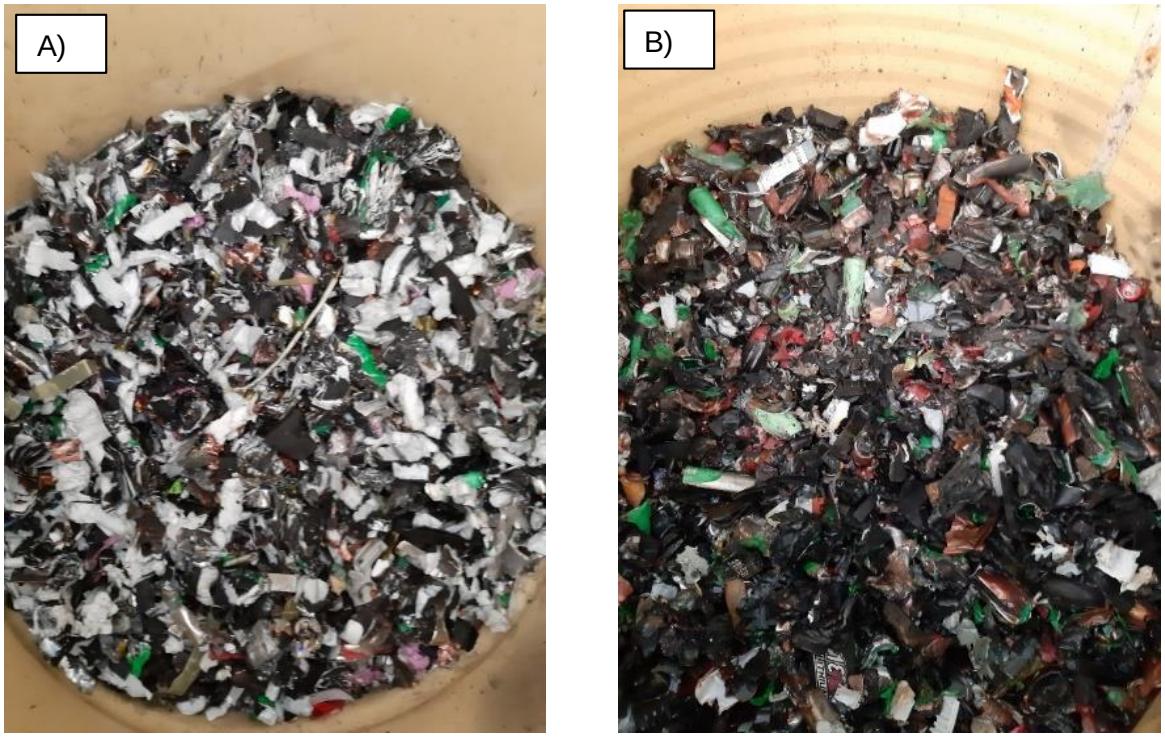

Figure 1: A) Sample from treatment of electronic bicycle batteries (e-bike sample). B) Sample from treatment of electronic tool batteries (power tool sample).

The release of possible harmful gaseous compounds from either of bulk samples was measured with Fourier Transform Infrared (FTIR) Gasmet Dx4000 which can simultaneously measure tens of gases and their concentrations. Measurements were done from the sealed sample containers (~150l). The containers were shaken to perturb the sample and any potential volatiles before the measurement. The measurement was done by pumping the gas from the headspace of the containers through the holes drilled to the lid. The measurement was continued until the readings stabilised.

After the gas measurements, the bulk samples were then divided into sub-samples by employing quartering and coning technique. In the technique after each quartering, opposite quarters are merged and half of the sample is discarded leaving the other half for the next quartering. This procedure is carried out until the desired sub-sample size is reached, in our case ca. 5 kg. The 5 kg sub-sample was used in particle size distribution determinations after which gas measurements were conducted on selected size fractions. Finally, composition analysis in various particle size fractions were performed namely XRF on fines (<2 mm) and hand sorting on coarse particles (>4 mm). A schematic description of the study procedures can be seen in Figure 2.

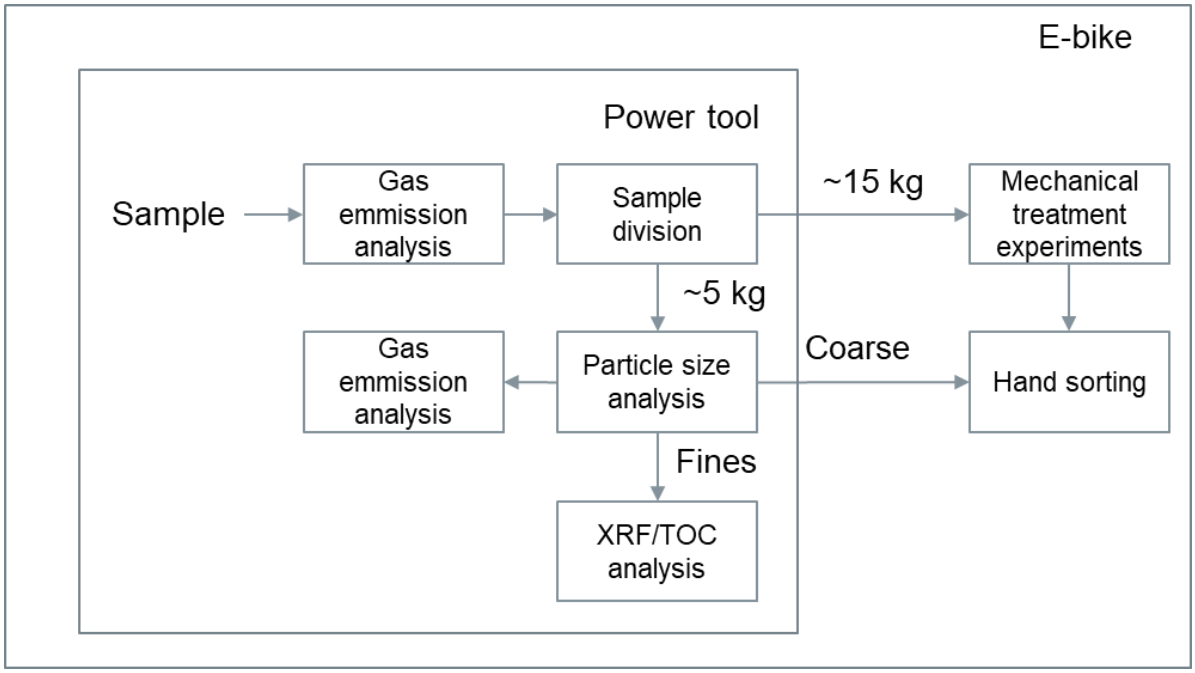

Figure 2. A schematic description of the procedures carried out on both E-bike and Power tool sample.

Size Fraction Analyses

For the determination of particle size distribution, a 5 kg subsample was sieved to 12 size fractions (0,5 - 63 mm sieves by using a vibrating sieve machine (Retsch AS300 Control). The particle size distribution was determined for both the E-bike as well as the power tool sample. Selected size fractions from both samples were measured again with Gasmet Dx4000 prior to the further handling to investigate if greater emissions can be detected on certain size fractions. For measurement the sieved samples were placed in sealed container (~10 L). The measurement was done by pumping the gas from the headspace of the containers through the holes drilled to the lid. The measurement was continued until the readings stabilised. After gas emissions studies, the finer particles (< 2 mm) were analysed for chemical composition, and the coarser size fractions (> 4 mm) were qualitatively sorted by hand.

Finer fractions composition of E-bike (<0.5 mm – 2 mm) were subcontracted and determined with XRF (Panalytical Axios mAX 3 kW). The composition of < 2 mm E-bike material was calculated via sum of the relative element fractions in each size fraction, weighted by mass of each size fraction. For power tool, the determination was done on <0.5 mm size fraction only. For both samples, the size fraction of <0.5 mm was analysed for total carbon, composed of total inorganic carbon and total organic carbon. The carbon analyses were subcontracted from Eurofins Ahma Oy, who conducted the investigation with SKALAR PRIMACS100 -TOC-analyser according to the standard SFS-EN 13137. To measure total carbon (TC) content, the sample was incinerated in 1100 °C with catalytic material using oxygen as a carrier gas. Released carbon dioxide is measured with infrared detector. Total inorganic carbon (TIC) is measured by adding phosphoric acid to sample and heating the mixture to 110 °C. Released carbon dioxide is measured with IR detector. Total organic carbon (TOC) is calculated from TC content by subtracting TIC content.

The coarser size fractions (> 4 mm) were then hand-sorted to qualitatively determine the presence of different material groups, as well as observe attach/detach behaviour. Samples were sorted to 24 different material groups (Table 1) composed of main groups (Al, Fe, Cu, Separators, PCB and electronics, Paper and cardboard, Plastics, Al foils, Cu foils,

Elastomer/rubber, battery cells, fines, wires). Based on these main groups, combinational categories were also created when it was not possible to distinguish individual material classes from a single massive particle or piece, for instance groups like Al + other, Separators + active material and so on were formed. Material group of each particle was qualitatively determined. For example, if a particle contained aluminium and plastic, the decision whether it was classified as *Al + other* or *Plastic + metal* was based on the performers understanding of which substance is greater in mass on particle in question. All size fractions were sorted by the same researcher to maintain consistency in the decision-making of the sorting throughout the project. Fraction "*Battery cells damaged*" contained damaged battery cells and pieces of battery cells where anode, cathode, separators and casing material of cells were visible, whereas fraction *"Battery cells (cat + ano + sep)"* consisted of pieces of battery cells with anode, cathode and separators without casing materials. Pieces that were found too small to be hand sorted were classified as "Fines".

Table 1. Example of a table for hand sorting.

Sieve size (mm)	63	31,5	20	14	10	8	5,6	4	2	1	0,5
Mass (g)											
Material group (g)											
Fe											
Fe + other (plastic etc.)											
Al											
Al + other (plastic etc.)											
Cu											
Cu + other (plastic etc.)											
Separators (plastic film)											
Separators + active material											
PCB + electronics											
PCB + other (plastic etc.)											
Paper & cardboard											
Plastic (films other)											
Plastic (black)											
Plastic (other color)											
Plastic + metal											
Al foil											
Al foil + active material											
Cu foil											
Cu foil + active material											
Elastomer/rubber											
Battery cell (damaged)											
Battery cell (cat + ano + sep)											
Fines											
Wires + other											
Sum	0	0	0	0	0	0	0	0	0	0	0

Magnetic and Eddy-Current Separation

For eddy-current and magnetic separation studies, the remaining 15 kg E-bike sample was sieved into two fractions: fine (< 4mm) and coarse (> 4 mm). The coarse size fraction was then subjected to magnetic separation and eddy-current experiments.

Coarse fraction (>4 mm) was separated to magnetic and non-magnetic fractions using magnetic drum separator (ERIEZ RR 305.300) with drum speed 6 and feed rate 3. Sieving with 4 mm was repeated after magnetic separation. Sieved non-ferrous fraction (>4 mm) was then separated with eddy current separator (ERIEZ Rev X-E NM-ST22-12) to three fractions namely; inner box, middle box and splitter which is the most outward box (Figure 3). The boxes and splitter level were adjusted to reach best possible separation of anode and cathode materials. The resulted fractions were then split to obtain representative subsamples, which were visually characterised (hand-sorted) in similar manner as the initial e-bike sample with the exception of having only five material/component groups namely; Al-foil (incl. active

material), Cu-foil (incl. active material), plastic, battery cells and other, to determine the efficiency of the tested treatment.

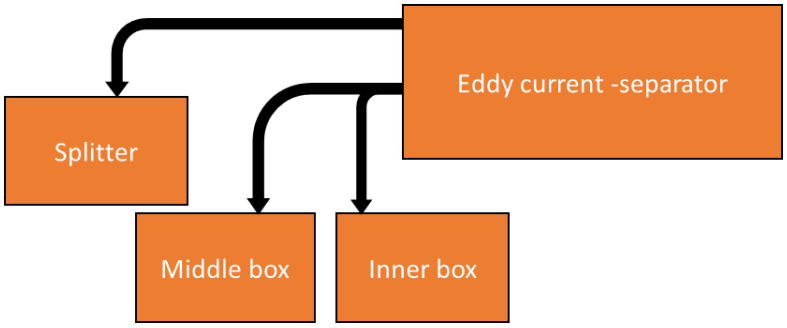

Figure 3. Approximate positioning of the boxes of eddy current separator.

Results and Discussion

Size Classification

Size classification was carried out to ascertain whether selective separation of any particular component would be possible as well as identify possible differences in breaking characteristics. Initially, the whole samples were analysed for size. The measurements were done by sieving, and the cumulative particle size distribution as (wt.%) for both the bike and the power tool battery is shown in Figure 4. Both samples were reasonably similar to each other in distribution, with the e-bike sample containing slightly more smaller pieces than the power tool. Conversely, the reverse was true for larger fractions. The similarity of the samples, and hence probably the similar behaviour in the crushing that was done before material delivery: median particle size is similar for both e-bike and power tool battery (16.5 vs 17.5 mm, respectively). The D10, D50 and D90 values are shown in Table 2. The differences between the behaviour of material is not huge, and no estimate of variation can be provided due to raw material batches being limited to one. Any unaddressed bias, such as the one introduced by quartering or natural variation in the crushing, could potentially explain the difference.

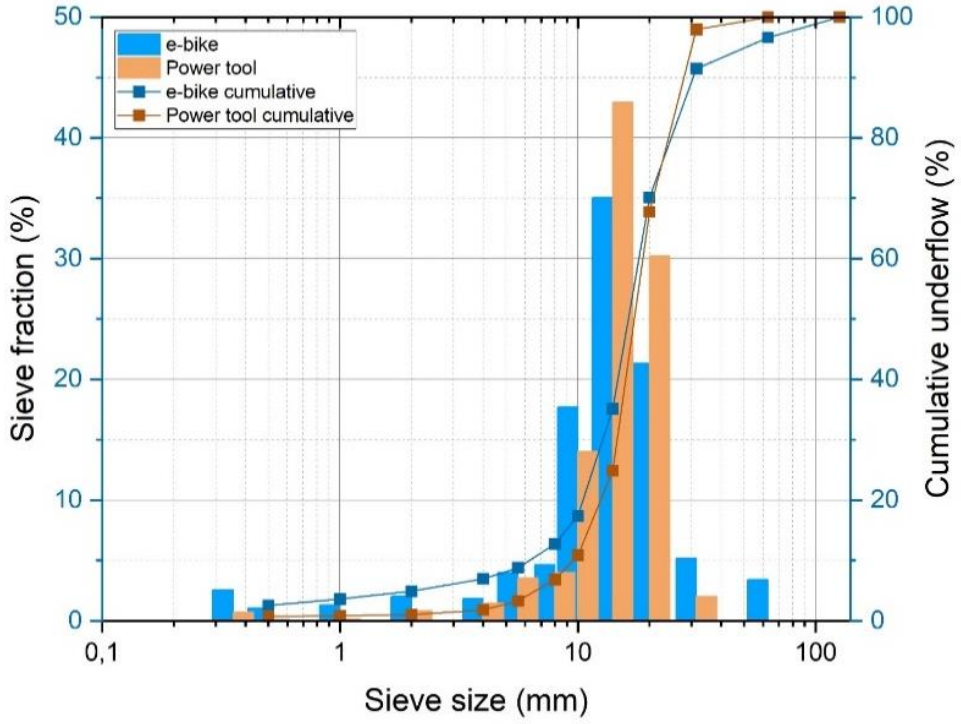

Figure 4. Particle size distribution of the samples

Table 2. Key parameters of the particle size distribution

Particle size parameter	E-bike sample	Power tool sample
d_{10}, mm	6,33	9,57
d_{50}, mm	16,5	17,5
d_{90}, mm	25,3	28,5

Material Composition and Distribution

After these treatments the power tool sample was discarded, and apart from the gas measurements, the focus of the study remained with the E-bike sample. Following the size classification, the different size classes were both characterized chemically (by XRF) and classified visually (by hand). The final calculated XRF results for E-bike sample is presented in **Error! Reference source not found.**. Evidently, the composition indicates that most of the materials consists of the active materials – *ca.* 37 wt.% of the mass is Ni, Co or Mn. Although not analysed, Li should account for roughly 1/10 of the wt.% of the sum of Ni, Co and Mn as the molar mass of Li (6.941 g/mol) is very roughly slightly more than one tenth of Ni, Co or Mn molar mass (58.69, 58.93, 54.94, respectively), and each mol of Ni, Co and Mn should correspond to 1 mol of Li. In addition, carbon (i.e. at least partially, graphite) content was analysed. Based on TC analysis, the total carbon content was found to be around 40-45%, which in part should be due to the anode graphite. Winslow et al. estimated that *ca.* 20 wt.% of a cell is composed of anode active material [13]. Presence of P can be explained by electrolyte salts ($LiPF_6$ and its derivatives in particular). Similarly, Al could be indicative of shredded Al foil pieces. Si and Br could potentially be from PCB.

Table 3: Final XRF analysis results for the particles in E-bike and power tool batteries: E-bike results are composed of three sieve sizes (<0.5 mm, 0.5-1 mm and 1-2 mm. Power tool result is based on <0.5 mm size class only.

Element	Al %	Si %	P %	S %	Cl %	Mn %	Fe %	Co %	Ni %	Cu %	Br %
E-Bike	2.7	0.3	3.8	0.6	0.1	12.5	6.2	12.8	10.7	20.4	0.12
Power Tool	3.6	1.6	2.7	0.29	0.11	12	9.1	9.1	22	7.2	0.11

The classification of the components was done for size classes larger than 4 mm. In Figure 5, the distribution of different components into individual size classes are broken down. In addition, in Figure 6, the graph is reversed to elaborate what was the composition of each size class.

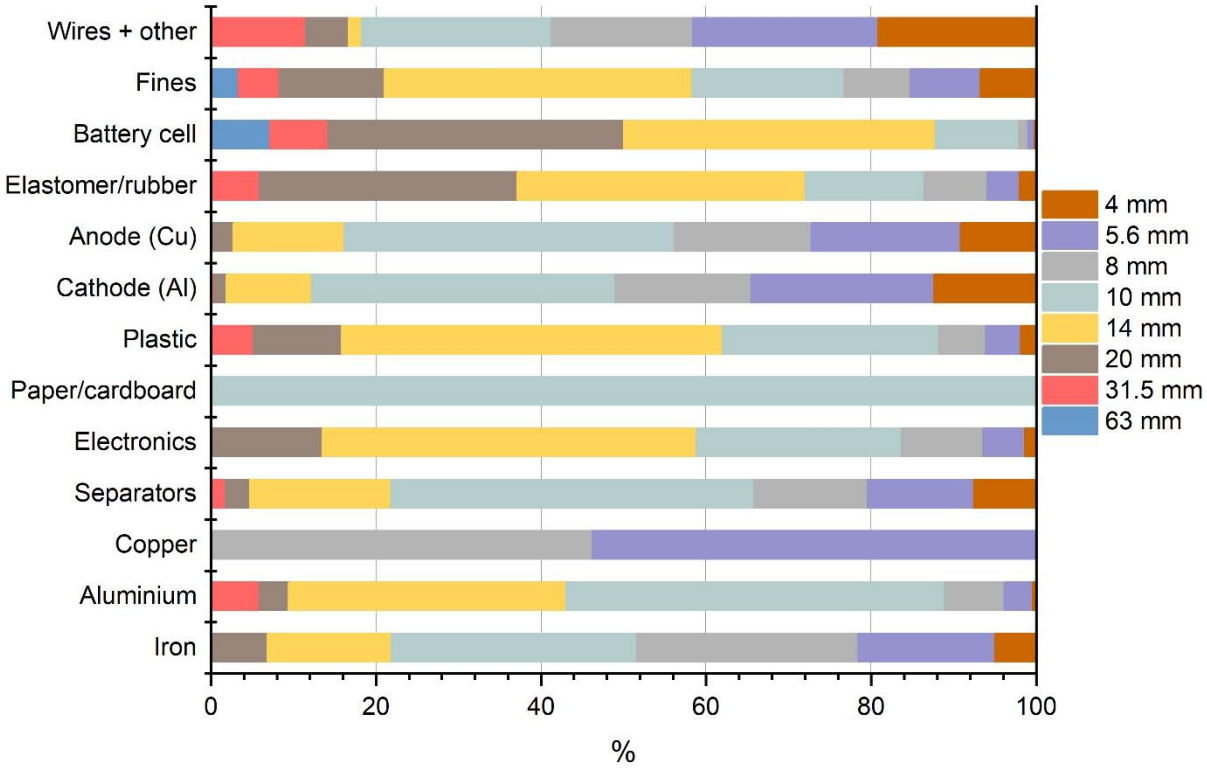

Figure 5: Material distribution into each different size class > 4 mm.

For instance, the Cu anode and Al cathode foils are mostly concentrated to size classes < 10 mm. Similarly, iron which originates mostly from the cell casing concentrates under 10 mm indicating that when the battery cell is broken in the crusher, different components start to separate under 10 mm. Only battery cells were in the overflow of 63 mm sieve, and the rest of the materials, along with part of the cells, went into the underflow. Plastics could be found in most of the size classes. Fine powders and separator materials could be observed to be present in a significant weight fractions in 4.0, 5.6 and 8.0 mm size classes, signifying potential valuable and hazardous material losses in size-based separation.

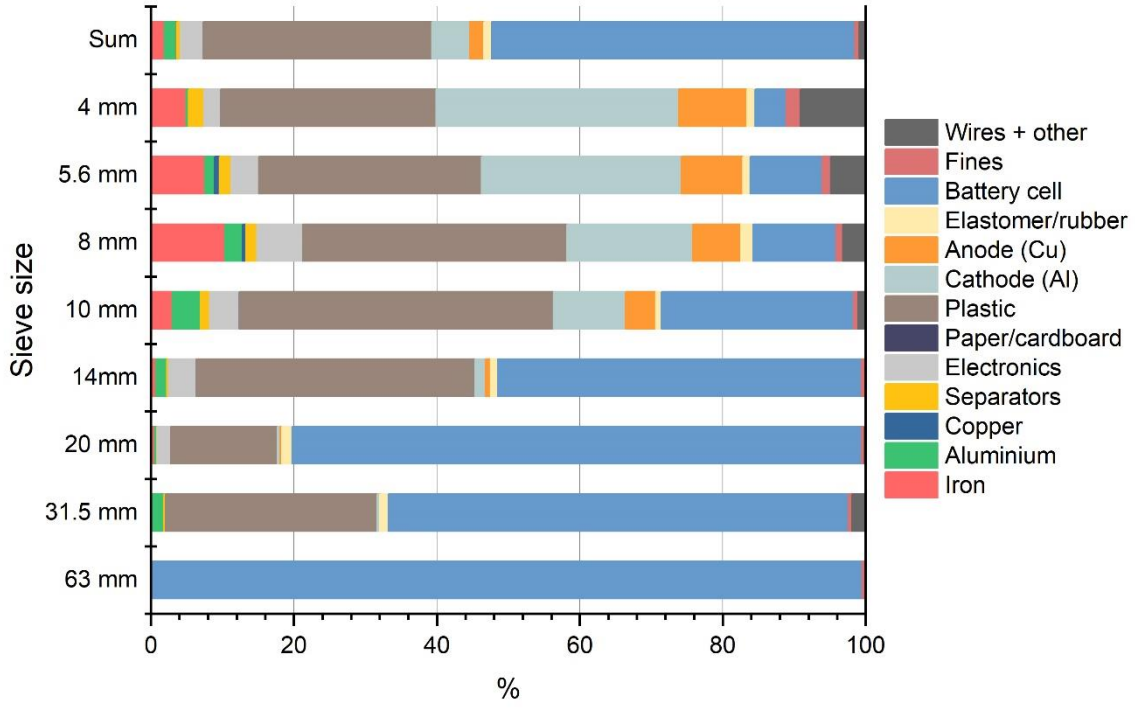

Figure 6: The distribution of different particle types in different size classes above 4 mm, as well as the sum of different components overall.

The liberation of Al and Cu was also investigated. The study indicated that most of the Al foils throughout the size classes which were larger than 4 mm were still mainly coated, i.e. not liberated. This is not surprising as PVDF has been commonly used there as a binder, although recent reports indicate that water-soluble and fluoride-free alternatives, such as carboxymethyl cellulose (CMC), are being investigated [14]. Similarly, the anode Cu foils had most of what was assumed to be the coating, and only *ca.* 10% foils were clean. This may indicate different detach behaviour of active materials between anodes and cathodes. In terms of liberation it was also observed that intact battery cells remained after the primary crushing that was performed by the raw material provider.

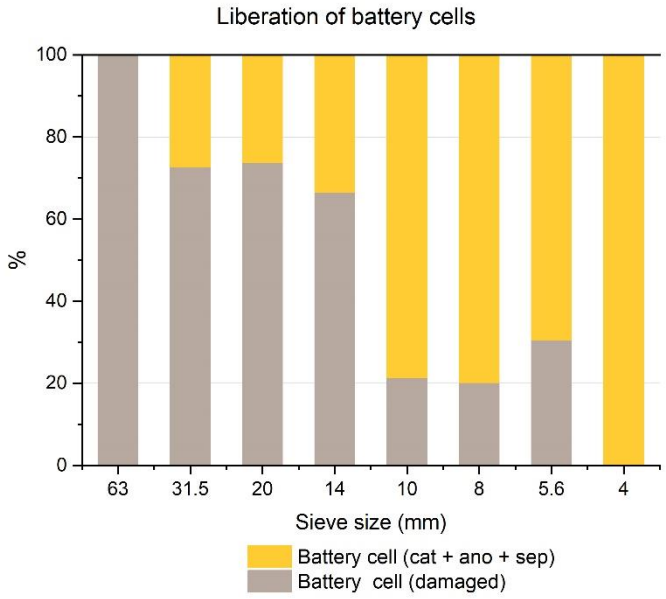

Figure 7: Qualitative separation of damaged battery cells vs. cells with liberated contents

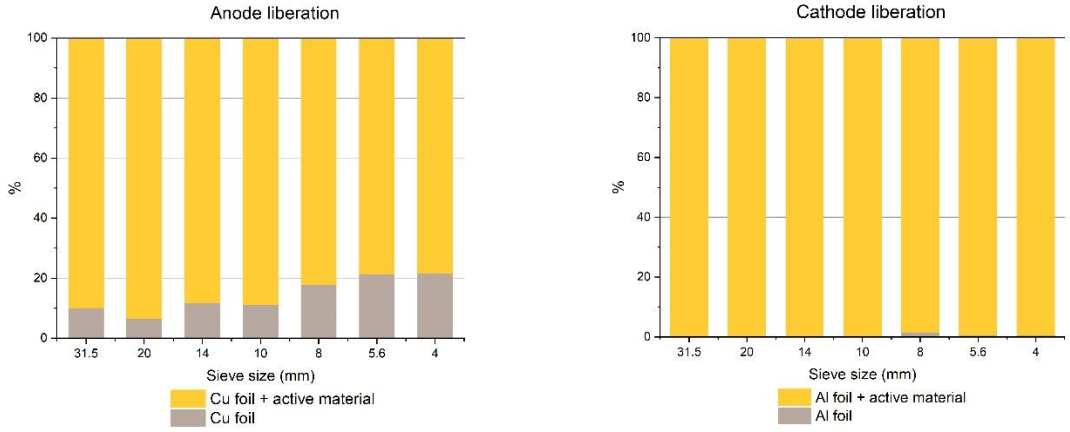

Figure 8 Liberation characteristics of cathode and anodes.

The impure foils are presented below in Figure 9. Either a complete layer, or part of it, remains on both Cu foils as well as Al foils. Superficially, it was observed that Cu foils were less impure than the Al foils, indicating a difference in attachment behaviour of the foils. This problem of binder attachment is well-known.

Figure 9: Impure Cu and Al foils, upon which active electrode materials still reside.

It needs to be noted as well that these foils do appear to break apart, even after size-based separation, which would support the assertion of why Cu and Al are found in the XRF analysis of finer fractions. Further 'fine' fractions were generated during the hand-sorting and manipulation of the materials, as shown in Figure 10.

Figure 10: Further fines, composed of graphite, metal oxides and foils pieces, generated from the size class of 4-5.6 mm.

Gas Measurements

The different size fractions were subjected to gas measurements. As the raw material provider had not done, apart from crushing, any other mechanical treatments for the raw materials, it was prudent to investigate potential emissions from the raw materials. Secondary Li-ion

batteries contain organic solvents as the electrolyte. Furthermore, decomposition and oxidation products may also be detected, such as CO_2. It needs to be noted that the analyses were performed in atmospheric gas: *ca.* 400 ppm is the expected atmospheric CO_2 concentration and the baseline the results should be related to this. In the case of organic carbonates concentrations, ranging between *ca.* 15 – 105 ppm, were detected throughout the different size fractions. For instance, dimethyl carbonate has an exposure limit of *ca.* 34.9 mg/m3 for a daily continuous exposure as per CarlRoth's material safety datasheet. In this case, information about exposure limits were not generally available, for instance European Chemicals Agency database lacked any exposure limits, although the substance was listed on hazardous substances list. As for lower explosion limits, which can be relevant in the crushing stage of battery waste, according to Sigma Aldrich´s material safety data sheet on dimethyl carbonate has the lower limit at 4.22 vol-%. Regardless, these emissions could be indicative of the separator membranes being present in each of the size fractions. Emissions for HF were also checked, but none was detected. It was hypothesized that evolution of gaseous HF could be possible, assuming unreacted $LiPF_6$ or its hydrolysed products were still present in the raw material. Although no emissions were detected, care should be practiced if the operator is unsure of the potential as $LiPF_6$ is known to react with moisture and heat [15].

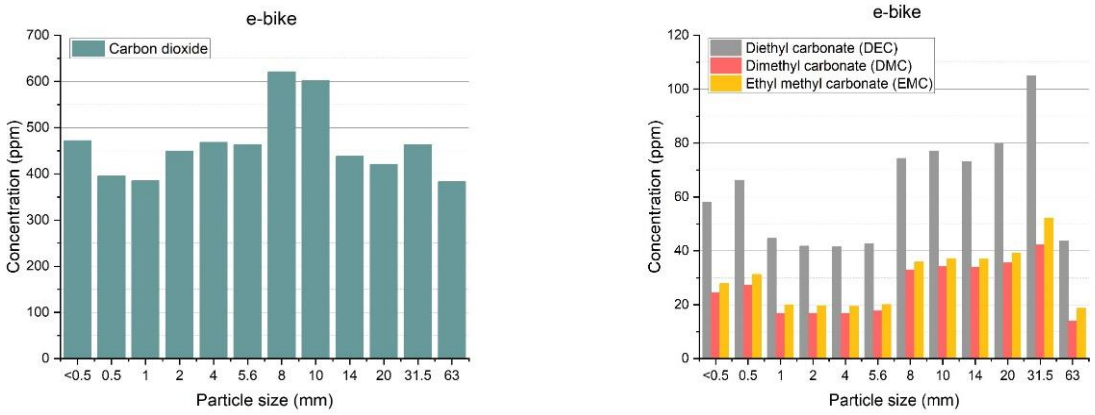

Figure 11. Left side: measured CO_2 concentrations from the barrel. Ca. 400 ppm is the baseline. Right side: DEC, DMC and EMC concentrations from different sieve fractions of the e-bike sample.

Magnetic and Eddy-Current Separation

As the presence of fine material in magnetic and eddy current separation can affect their separation efficiency and the decreasing separation efficiency for eddy current separator when going below 4 mm the, the sample, a total of 16500 g, was first sieved with a 4 mm sieve. 6.6 wt.% of the original sample was size separated in this manner, corresponding to 1025 g of fine materials. In magnetic separation, 5701 grams of the material was found to be magnetic and 9430 grams non-magnetic. The magnetic fraction composed mostly, with over 85 w-%, of damaged battery cells which magnetic casings originated the separation property. Around 64 % of cells were separated to this fraction. The non-magnetic fraction was then subjected to eddy-current separation.

Before eddy-current separation, but after magnetic separation, the magnetic and nonmagnetic fractions were sieved once more with 4 mm and 1 mm sieves. This was carried out since particles collide and grind against each other and the equipment surfaces at which time fine material detach for example from the foils. In the magnetic fraction, consisting of 5701 grams, 0.9 wt.% of the mass was separated into fines. For the non-magnetic fraction, 2.3 wt.% of the 9430 gram sample had particle size < 4 mm which was separated into fines. This highlights the importance of considering ways of liberating the fines from the foils. The result is not

surprising considering that visual inspection showed that most Al foils present were still adhered to powders.

In eddy-current separation, the mass distribution within the three fractions namely the inner box, middle box and splitter which is the most outward was 8.6 wt.%, 75.9 wt.% and 15.5 wt.% respectively. The total mass of the treated sample was 9158 g. Losses amounted to 24.8 g or 0.27 wt.%.

When observing the composition in the fractions (Figure 12) it can be noticed that both Al- and Cu foils including active material enriched with the content of 18 wt.% and 6 wt.% and the recovery of 28 % and 32 % respectively to the splitter fractions. When comparing to the content of the components in the feed, the content is around three times. However, both foils were detected also in the other two fractions and when reflecting to the mass distribution of the fractions, over half of foils are lost especially to the middle fraction even though the concentrations are low. One potential reason for this is the shape of the particles, since particles which one dimension is substantially smaller than the other ones such as foils the air resistance may affect the particles trajectory in a such a way that it won't reach the splitter fraction.

As for the plastic particles, which are non-conductive, a circulating eddy current is not generated and as a result a separating force bouncing the particle is not generated. Therefore, these particles continue with the trajectory which they have at the end point of the belt. Of course the air resistance and gravity affects the trajectory. Consequently, 93 wt.% of plastic particles end to the middle fraction making it the prevailing material in it.

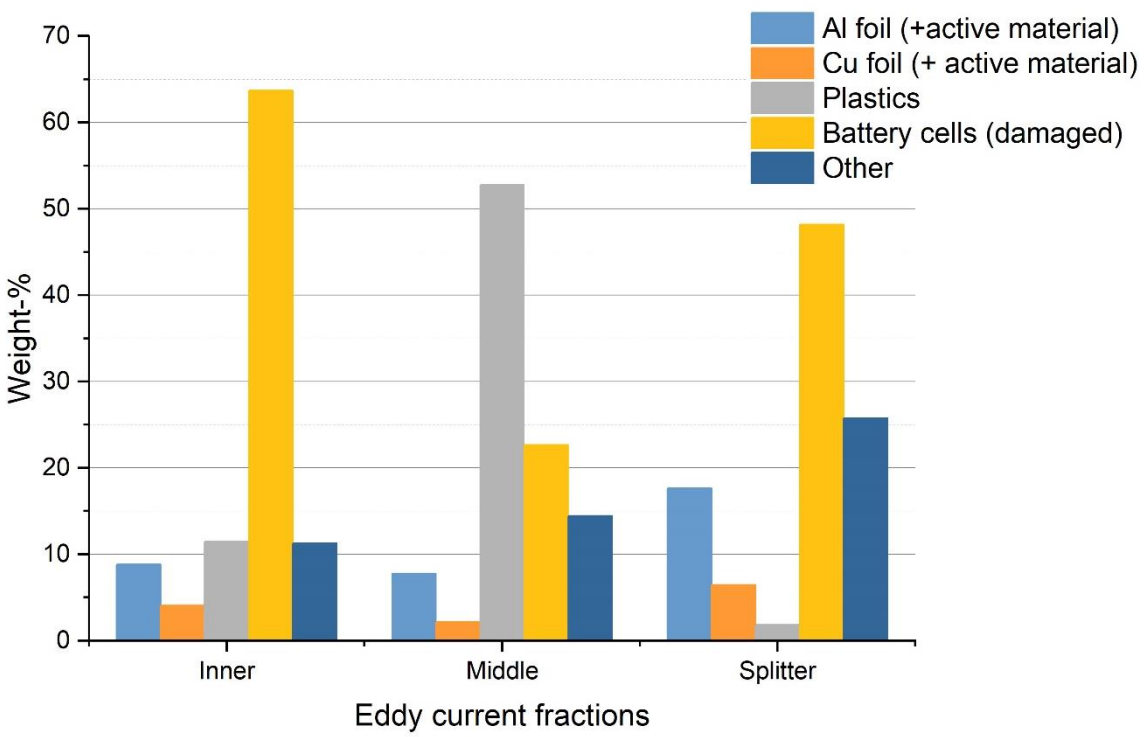

Figure 12. The component composition in the three fractions produced in the eddy current separation.

Interestingly, the damaged battery cells was observed in higher contents both in the inner box and splitter fractions. As for the high content in the inner box fraction, weakly magnetic particles has been reported to remain fasten on the rotor and move thus to the inner box [16]. These

battery cells may still contain weakly magnetic parts. As for the damaged battery cells in the splitter fractions, these do not any more contain magnetic parts at which time both the Al and Cu in the cell generate the eddy current and consequently the separating force. In addition, aluminium casing in the cell enhance the separation. When reflecting this observation with the behaviour of Al- and Cu foil, the recovery anode and cathode increases notably.

As for others, they end in all fractions but in higher content to the splitter fraction. This fraction compose mainly of aluminium casing particles which have liberated from the cell during the crushing stage. Possible electronic parts such as printed circuit boards tend also to burst further due to their Cu-lamination.

It should be noticed that as the feed had only undergone the primary crushing stage which aim is not to generate optimal feed including among other things liberated components and narrow article size distribution for eddy current, these results are more indicative. For investigation more actual applicability of eddy current separation for battery waste, further experiments with secondary crushed battery waste would be valuable.

Conclusions

In this task, VTT had the research questions pertaining to safe handling and pre-treatment of spent battery cells (E-bike and power tool batteries) that had only undergone primary crushing. Two different, primary crushed samples were obtained. The off gassing of the material after a period had gone from primary crushing was investigated by means of FTIR and HF detectors. No HF was detected, however, some residual organic gaseous emissions, including CO_2, were detected. Although no HF emissions were detected, care should still be practiced in handling the materials due to the potential, unreacted LiPF6 or its intermediate reaction products being present in the materials. After emission tests, and size-separation, the power tool sample was discarded, and the study was refocused on the E-bike sample. The e-bike sample was visually classified into components (> 4 mm size fraction). Classifications were performed on multiple basis: impure foils, undamaged cells, plastics, fines and so on. Some variation in active material release from cathode and anode was identified, as the graphite on anode Cu foils was detected in the qualitative sorting to be more loosely attached than the metal oxide powder on cathode Al foils. The underflow (< 4 mm fractions) were analysed by XRF, and the analysis revealed a presence of NMC chemistry with stoichiometric composition of NMC-111. The fines contained small quantities of Cu and Al (most likely from the foils) as well as P. Finally, magnetic separation and eddy-current separation of non-magnetic fractions were performed. Significant share of damaged battery cells was removed with magnetic separation whereas cathode and anode as well as plastics continued to eddy current separation. Eddy current abled to enrich some anode and cathode particles to splitter the outermost box. However, the recoveries were somewhat low. On the other hand, when taking into account the ability of separating damaged battery cells containing solely of anode, cathode and separator the recoveries increase significantly. As the sample had gone through only a primary crushing stage the feed was not the most optimum for the eddy current separation, which affects the separation efficiency. Further investigation with other designed batteries such as pouch and prism would be valuable. In addition, in future the crushability of different batteries would be as well an important research topic.

Acknowledgement

This study was funded by BATCircle project, grant number 5912/31/2018, supported by Business Finland. The raw material was provided by AkkuSer.

References

[1] "EUR-Lex - 52020DC0474 - EN - EUR-Lex." .

[2] J. Diekmann *et al.*, "Ecological recycling of lithium-ion batteries from electric vehicles with focus on mechanical processes," *J. Electrochem. Soc.*, vol. 164, no. 1, pp. A6184–A6191, 2017.

[3] S. Al-Thyabat, T. Nakamura, E. Shibata, and A. Iizuka, "Adaptation of minerals processing operations for lithium-ion (LiBs) and nickel metal hydride (NiMH) batteries recycling: Critical review," *Miner. Eng.*, vol. 45, pp. 4–17, 2013.

[4] A. Porvali *et al.*, "Mechanical and hydrometallurgical processes in HCl media for the recycling of valuable metals from Li-ion battery waste," *Resour. Conserv. Recycl.*, vol. 142, pp. 257–266, Mar. 2019.

[5] G. Harper *et al.*, "Recycling lithium-ion batteries from electric vehicles," *Nature*, vol. 575, no. 7781, pp. 75–86, 2019.

[6] E. Fan *et al.*, "Sustainable Recycling Technology for Li-Ion Batteries and Beyond: Challenges and Future Prospects," *Chem. Rev.*, 2020.

[7] R. Sommerville, J. Shaw-Stewart, V. Goodship, N. Rowson, and E. Kendrick, "A review of physical processes used in the safe recycling of lithium ion batteries," *Sustainable Materials and Technologies*, vol. 25. Elsevier B.V., p. e00197, Sep-2020.

[8] J. Ordoñez, E. J. Gago, and A. Girard, "Processes and technologies for the recycling and recovery of spent lithium-ion batteries," *Renewable and Sustainable Energy Reviews*, vol. 60. pp. 195–205, 2016.

[9] D. Song, X. Wang, E. Zhou, P. Hou, F. Guo, and L. Zhang, "Recovery and heat treatment of the Li(Ni1/3Co 1/3Mn1/3)O2 cathode scrap material for lithium ion battery," *J. Power Sources*, vol. 232, pp. 348–352, Jun. 2013.

[10] M. Contestabile, S. Panero, and B. Scrosati, "A laboratory-scale lithium-ion battery recycling process," *J. Power Sources*, vol. 92, no. 1–2, pp. 65–69, 2001.

[11] C. Hanisch, T. Loellhoeffel, J. Diekmann, K. J. Markley, W. Haselrieder, and A. Kwade, "Recycling of lithium-ion batteries: a novel method to separate coating and foil of electrodes," *J. Clean. Prod.*, vol. 108, Part, pp. 301–311, Jan. 2015.

[12] C. Hanisch, W. Haselrieder, and A. Kwade, "No Title," 2017.

[13] K. M. Winslow, S. J. Laux, and T. G. Townsend, "A review on the growing concern and potential management strategies of waste lithium-ion batteries," *Resources, Conservation and Recycling*, vol. 129. Elsevier B.V., pp. 263–277, Feb-2018.

[14] D. L. Thompson *et al.*, "The importance of design in lithium ion battery recycling-a critical review," *Green Chemistry*, vol. 22, no. 22. Royal Society of Chemistry, pp. 7585–7603, Nov-2020.

[15] M. D. S. Lekgoathi, B. M. Vilakazi, J. B. Wagener, J. P. Le Roux, and D. Moolman, "Decomposition kinetics of anhydrous and moisture exposed LiPF6 salts by thermogravimetry," *J. Fluor. Chem.*, vol. 149, pp. 53–56, May 2013.

[16] F. Settimo, P. Bevilacqua, and P. Rem, "Eddy current separation of fine non-ferrous particles from bulk streams," *Phys. Sep. Sci. Eng.*, vol. 13, no. 1, pp. 15–23, Mar. 2004.